Dual role of the exocyst in AMPA receptor targeting and insertion into the postsynaptic membrane

Nashaat Z. Gerges[1], Donald S. Backos[1], Chamila N. Rupasinghe[2], Mark R. Spaller[2] and José A. Esteban[1,*]

[1]Department of Pharmacology, University of Michigan Medical School, 1150 W Medical Center Dr., Ann Arbor, Michigan 48109-0632. [2]Department of Chemistry, Wayne State University, Detroit, Michigan 48202.

Running title: Exocyst in AMPA receptor synaptic trafficking

Subject Categories: Neurosciences, Membranes & Transport

Character count: 59,834

*Correspondence: estebanj@umich.edu

ABSTRACT

Intracellular membrane trafficking of glutamate receptors at excitatory synapses is critical for synaptic function. However, little is known about the specialized trafficking events occurring at the postsynaptic membrane. We have found that two components of the exocyst complex, Sec8 and Exo70, separately control synaptic targeting and insertion of AMPA-type glutamate receptors. Sec8 controls the directional movement of receptors towards synapses through PDZ-dependent interactions. In contrast, Exo70 mediates receptor insertion at the postsynaptic membrane, but it does not participate in receptor targeting. Thus, interference with Exo70 function accumulates AMPA receptors inside the spine, forming a complex physically associated, but not yet fused with the postsynaptic membrane. Electron microscopic analysis of these complexes indicates that Exo70 mediates AMPA receptor insertion directly within the postsynaptic density, rather than at extrasynaptic membranes. Therefore, we propose a molecular and anatomical model that dissects AMPA receptor sorting and synaptic delivery within the spine, and uncovers new functions of the exocyst at the postsynaptic membrane.

Keywords: membrane trafficking/synaptic plasticity/hippocampus/Exo70/Sec8

INTRODUCTION

The exocyst is a multiprotein complex originally described in yeast to be required for exocytosis (TerBush et al., 1996). It consists of eight different subunits (Sec3, Sec5, Sec6, Sec8, Sec10, Sec15, Exo70 and Exo84), whose mammalian counterparts have been already identified (Hsu et al., 1996; Kee et al., 1997; Ting et al., 1995). The exocyst is localized at the plasma membrane and intracellular compartments (Shin et al., 2000; Yeaman et al., 2001), and it associates with cytoskeletal elements involved in vesicular trafficking (Hsu et al., 1998; Shin et al., 2000; Vega and Hsu, 2001; Wang et al., 2004). The exocyst is broadly expressed in adult brain and is enriched in synaptic membranes (Hsu et al., 1996; Sans et al., 2003; Vik-Mo et al., 2003). However, its role in neurons has always been associated with membrane trafficking events required for neuronal development, such as neurite outgrowth (Vega and Hsu, 2001), synaptogenesis (Hazuka et al., 1999) and dendritic trafficking of newly synthesized NMDA receptors (NMDARs) (Sans et al., 2003). In contrast, the functional role of the exocyst in established synapses remains unclear.

Synaptic function is critically dependent on the targeting and delivery of a large number of different proteins at the postsynaptic membrane, including neurotransmitter receptors, ion channels, anchoring and cell adhesion molecules, and a variety of signal transduction modulators (Garner et al., 2000; Kim and Sheng, 2004; McGee and Bredt, 2003; Yamagata et al., 2003). AMPA type-glutamate receptors (AMPARs) mediate most excitatory synaptic transmission in the brain. Nevertheless, they are highly dynamic components of excitatory synapses. AMPARs can be added to or removed from synapses in an activity-dependent manner, leading to long-term potentiation (LTP) or depression (LTD) of synaptic transmission (see (Barry and Ziff, 2002;

Bredt and Nicoll, 2003; Esteban, 2003; Malinow and Malenka, 2002; Sheng and Lee, 2001) for recent reviews). In addition to this regulated trafficking, AMPARs continuously cycle in and out of synapses in an activity-independent manner, which requires NSF (Luscher et al., 1999; Nishimune et al., 1998; Song et al., 1998), Hsp90 (Gerges et al., 2004b) and NEEP21 (Steiner et al., 2005) function. Multiple proteins have been described to interact with AMPAR subunits and affect their synaptic localization (see (Henley, 2003; Kim and Sheng, 2004; Scannevin and Huganir, 2000) for recent reviews); however, we still know very little about the membrane trafficking mechanism mediating AMPAR targeting and delivery into synapses.

Here we have explored a potential role for the exocyst in the dynamic behavior of AMPARs at the postsynaptic membrane. Using a combination of molecular biology, electrophysiology, fluorescence imaging and electron microscopy, we have found that different subunits of the exocyst mediate AMPAR synaptic trafficking at several distinct levels. Intracellular receptor targeting within the spine is mediated by the Sec8 subunit of the exocyst, possibly through PDZ-dependent interactions with synaptic scaffolding molecules. Independently from vesicle targeting, receptor insertion into the postsynaptic membrane requires the Exo70 subunit. By separately manipulating vesicle targeting and receptor insertion, we now show that AMPAR synaptic delivery occurs from intracellular compartments within the spine directly into the postsynaptic density. Therefore, in addition to characterizing the exocytic machinery that operates at the postsynaptic membrane, these results delineate the subcellular pathways by which AMPARs reach their synaptic targets.

RESULTS

Different components of the exocyst play distinct roles in synaptic transmission

The C-terminus of the exocyst subunit Sec8 contains a PDZ motif that interacts with the synaptic scaffolding proteins PSD95 and SAP102 (Riefler et al., 2003; Sans et al., 2003) and is required for NMDAR trafficking (Sans et al., 2003). Therefore, as a first step to evaluate the role of the exocyst in synaptic transmission, we expressed the C-terminus (last 16 amino acids) of Sec8 as a GFP-fusion protein in CA1 hippocampal neurons from organotypic slice cultures using the Sindbis virus system (see Supplementary Information). This construct may act as a dominant negative by competing with the endogenous exocyst for its PDZ synaptic partners. The effect of Sec8 C-terminus (Sec8-Ct) on synaptic transmission was evaluated by simultaneous double whole-cell recordings from neurons expressing the recombinant protein and nearby uninfected neurons (Methods). As shown in Fig. 1A, Sec8-Ct significantly reduced AMPAR and NMDAR responses in hippocampal CA1 neurons, while $GABA_A$ receptor-mediated transmission remained unaffected. The depression of NMDA responses and lack of effect on $GABA_A$ responses are consistent with previously published observations using another Sec8 dominant negative construct (Sans et al., 2003). As control, overexpression of the full-length Sec8 protein (Sec8-wt) fused to GFP did not affect AMPA or NMDA transmission (Fig. 1B). Importantly, expression of a truncated form of Sec8-Ct lacking its last four amino acids (Sec8-Ct-Δ4), which are required for its PDZ interactions (Sans et al., 2003), did not alter AMPA or NMDA responses either (Fig. 1C). These results suggest that the dominant negative effect of Sec8-Ct is indeed due to competition for PDZ-binding domains, which would be required for the synaptic delivery or stability of both AMPARs and NMDARs.

Although both AMPARs (Bredt and Nicoll, 2003; Malinow and Malenka, 2002) and NMDARs (Nong et al., 2004; Perez-Otano and Ehlers, 2005; Prybylowski et al., 2005) undergo regulated synaptic trafficking, NMDARs are considered to be fairly stable components of the synapse, as compared with AMPARs (Sheng, 2001). Therefore, interference with a potential role of the exocyst specifically in receptor delivery is more likely to affect AMPARs to a larger extent than NMDARs. A truncated form of the exocyst subunit Exo70, lacking its C-terminal half (Exo70-N), has been recently shown to block the exocytic delivery of the glucose transporter Glut4 into the adipocyte cell surface (Inoue et al., 2003). Importantly, this truncated Exo70 is still able to interact with endogenous exocyst subunits (see Supplementary Fig. 1 and (Inoue et al., 2003)). We therefore evaluated the effect on synaptic transmission of Exo70-N as a GFP fusion protein in CA1 hippocampal neurons. As shown in Fig. 1D, AMPAR-mediated responses were significantly reduced in Exo70-N expressing neurons. Importantly, NMDAR responses were not affected, in contrast to the result obtained with Sec8-Ct. This result is also confirmed by the decrease in the ratio of AMPA to NMDA responses in Exo70-N-expressing neurons (Fig. 1D; to note, AMPA/NMDA ratios are intrinsically very variable across slices; therefore, comparisons between infected and uninfected cells were always drawn from recordings within the same slice, and in most cases, as simultaneous double recordings). As control, overexpression of full-length Exo70 (Exo70-wt) fused to GFP did not affect AMPA or NMDA synaptic responses (Fig. 1E). The differing effects of Exo70-N on AMPA and NMDA synaptic transmission suggest that the Exo70 subunit of the exocyst mediates receptor insertion at synapses, which is more likely to affect the continuous synaptic delivery of AMPARs than the stable presence of NMDARs at synapses. (To note, none of these wild-type and dominant

negative constructs affected passive membrane properties of the infected cell, such as input resistance and holding current; see Supplementary Fig. 2).

Sec8 PDZ-dependent interactions are required for the constitutive synaptic cycling of AMPA receptors

The activity-independent, continuous delivery of AMPARs into synapses was originally inferred from intracellular peptide infusion experiments, in which AMPAR-mediated synaptic transmission rapidly ran down when a specific peptide competing GluR2-NSF interactions was loaded in the recorded cell (Luscher et al., 1999; Nishimune et al., 1998). We have used the same approach to determine whether the PDZ motif of Sec8 participates in the constitutive cycling of AMPARs. To this end, we recorded AMPAR-mediated synaptic responses from CA1 hippocampal neurons while infusing them with one of three peptides: Sec8 C-t (last 8 amino acids of Sec8), NR2B C-t (last 8 amino acids of the NMDAR subunit NR2B, which also contains a PDZ ligand motif (Kornau et al., 1995; Niethammer et al., 1996)) and Sec8-mut C-t (last 8 amino acids of Sec8 with the PDZ ligand sequence –TTV mutated to –ATA) (see Supplementary Information and Supplementary Fig. 3). These experiments were carried out in a blind fashion, that is, the person carrying out the electrophysiological recordings and the analysis did not know which peptide was used in the experiment. As shown in Fig. 2, the peptide corresponding to the Sec8 C-terminus produced a fast run-down of synaptic transmission, similar to the one observed for the GluR2-NSF peptide (Gerges et al., 2004b; Luscher et al., 1999; Nishimune et al., 1998). Importantly, the peptide corresponding to the PDZ ligand sequence of NR2B did not affect AMPAR-mediated responses, suggesting that specific PDZ-dependent interactions of Sec8 are required for the continuous synaptic cycling of AMPARs. As control, the mutated Sec8 C-t

peptide lacking the PDZ motif did not affect synaptic transmission either. Fig. 2B indicates that the differences in run-down of synaptic transmission obtained with the three peptides are not due to systematic changes in access resistance during the recordings.

The exocyst associates with AMPA receptors in hippocampal synaptosomes

Our data shown above suggests that the exocyst may be directly involved in AMPAR synaptic trafficking. Therefore, we tested whether an exocyst/AMPAR complex is present in the brain. To this end we carried out immunoprecipitation experiments from hippocampal synaptosomes after Triton solubilization (see Supplementary Information; all immunoprecipitations were replicated in at least three independent experiments). As shown in Fig. 3A, immunoprecipitation of the exocyst subunits Sec8 or Exo70 co-precipitated AMPARs but not metabotropic (mGluR) receptors. As previously published (Riefler et al., 2003; Sans et al., 2003), the exocyst also co-precipitated the PDZ protein PSD95 (Fig. 3A).

The exocyst complex has been recently shown to associate with NMDARs through its interaction with synaptic anchoring proteins, such as PSD95 and SAP102 (Sans et al., 2003). However, AMPA and NMDA receptors do not appear to associate in hippocampal extracts (Sans et al., 2000; Wyszynski et al., 1999) (see also Fig. 3B). Therefore, we investigated whether the exocyst forms separate complexes with AMPARs and NMDARs at synaptic terminals. To this end, Triton-solubilized synaptosomal extracts from hippocampus were immunoprecipitated with anti-GluR2/3 (AMPARs) or anti-NR1 (NMDARs) antibodies (see Supplementary Information). As shown in Fig. 3B, the exocyst subunits Exo70, Sec8 and Sec6 co-precipitated predominantly with AMPARs, but only to low levels with NMDARs. This result supports the notion that the exocyst forms separate complexes with AMPARs and NMDARs.

A potential role for Sec8 but not for Exo70 in the dendritic trafficking of AMPA receptors

It has been recently described that the exocyst mediates the export into dendrites of newly synthesized NMDARs in primary neuronal cultures (Sans et al., 2003). In order to test whether the exocyst plays a similar role in the trafficking of AMPARs in hippocampal slices, we co-expressed a GFP tagged AMPAR subunit (GluR2-GFP), together with Exo70-N, Sec8 C-t or NR2B C-t (as control) tagged with a red fluorescence protein (Exo70-N-RFP, Sec8-Ct-RFP or NR2B-Ct-RFP; see Supplementary Information). The efficiency of AMPAR transport along dendrites was quantified from the intensity of GFP fluorescence along the main apical dendrite, after background subtraction (see Supplementary Fig. 4A). As shown in Fig. 4, the trafficking of GluR2-GFP into distal dendrites was virtually identical with or without co-expressed Exo70-N, indicating that the transport of AMPARs along dendrites does not require a fully functional Exo70 subunit. In contrast, the dendritic transport of GluR2-GFP was significantly impaired when co-expressing Sec8-Ct or NR2B-Ct (Fig. 4; see Supplementary Fig. 4B for a complete quantification of AMPAR dendritic distribution in the presence of Exo70-N, Sec8-Ct and NR2B-Ct). These results reinforce the interpretation that Exo70 and Sec8 play different roles in AMPAR trafficking: Exo70 probably mediates a local step in AMPAR synaptic delivery, whereas PDZ-dependent interactions of Sec8 or other proteins are required for efficient receptor transport and targeting (since both Sec8-Ct and NR2B-Ct impaired dendritic trafficking, the identity of these PDZ interactions cannot be determined from these experiments).

Morphological dissection of AMPA receptor delivery into the spine surface

In order to directly test a local role of the exocyst in AMPAR trafficking, we monitored the transport of AMPARs from the dendritic shaft into adjacent spines and their delivery into the

spine plasma membrane. To this end, we co-expressed GFP-tagged GluR1 with a constitutively active, untagged form of αCaMKII (truncated αCaMKII, or tCaMKII) to trigger its synaptic delivery (see Supplementary Information and (Hayashi et al., 2000)), with or without Exo70-N. Protein expression was allowed for 36 hours, then slices were fixed and the surface distribution of the recombinant receptor in CA1 hippocampal neurons was monitored by immunostaining using an anti-GFP antibody under non-permeabilized conditions (the GFP tag is placed at the extracellular, N-terminus of the receptor). The immunostaining was visualized with an infrared fluorophore (Cy5). This experimental approach allows us to independently monitor the total amount of receptor (GFP channel), the fraction exposed to the cell surface (Cy5 channel) and the presence of the exocyst dominant negative construct (RFP channel). The distribution of surface and total receptor in spines and dendrites was quantified by line plots of fluorescence intensity across spine heads and adjacent dendritic shafts (see Fig. 5A for representative examples of the quantification of GFP and surface immunostaining from dendrite-spine pairs with or without co-expressed Exo70-N). Surface ratios were then calculated as the ratio between the intensity of the Cy5 signal (surface receptor) and GFP signal (total receptor) after background subtraction (Brown et al., 2005; Gerges et al., 2004a). Importantly, this assay is internally normalized for immunostaining variability, because surface labeling is always acquired in pairs of spines and adjacent dendritic shafts. This also means that absolute changes in surface receptors at spines or dendrites cannot be evaluated, but only relative changes between the two compartments. Finally, spines are selected solely from their GFP image, so the analysis is done blind with respect to their surface immunostaining.

As shown in Fig. 5B (first panel), surface expression of GluR1-GFP was slightly higher in spines as compared to their adjacent dendritic shafts when the exocyst function is intact. In

contrast, Exo70-N led to a marked reduction in the amount of receptors that reach the spine surface, to the point that surface expression at spines became significantly lower than at dendrites (Fig. 5B, second panel). This effect can also be evaluated from the leftward shift in the cumulative probability distribution of spine-to-dendrite ratios in the presence of Exo70-N (Fig. 5B, third panel).

A reduction of surface expression at spines may be due to an impaired translocation of the receptor into the spine. This step can be evaluated from the total receptor distribution (GFP channel) at spines and adjacent dendrites. As shown in Fig. 5C (first panel), GluR1-GFP partitions equally between dendrites and spines in the absence of exocyst dominant negative constructs. In marked contrast, and to our surprise, Exo70-N led to a significant increase (almost doubling) in the amount of total receptor in spines as compared to dendrites (Fig. 5C, second panel) (this effect can also be appreciated from the rightward shift in the cumulative probability distributions in Fig. 5C, third panel). Therefore, the decrease in receptor surface expression produced by Exo70-N is accompanied by an enrichment of receptors at spines.

The next trafficking step after translocation into spines is receptor insertion at the spine plasma membrane. This process can be evaluated independently by calculating ratios of surface to total receptor (Cy5/GFP) at spines and dendrites. This approach normalizes receptor surface expression to the total number of receptors in each compartment, and therefore, it reflects the intrinsic efficiency of receptor delivery at the plasma membrane. As shown in Fig. 5D (first panel), surface ratios were slightly higher at spines than at dendrites when GluR1-GFP was co-expressed only with tCaMKII. On the other hand, blockade of Exo70 function with Exo70-N strongly impaired receptor insertion at the spine surface, as judged from the drastic reduction in the surface ratio at spines versus dendrites (Fig. 5D, second and third panel).

These results support our interpretation that Exo70 plays a late step in AMPAR trafficking, even within the local environment of the synapse. Specifically, Exo70 seems to be required for the fusion of AMPAR-containing vesicles with the spine plasma membrane.

Interestingly, the accumulation of GluR1-GFP at intracellular compartments within the spine when Exo70 function is impaired, also suggests that this pool of AMPARs reaches the synaptic membrane from intracellular compartments contained within the spine. We then tested whether a similar intra-spine pathway is followed for the constitutive synaptic delivery of the cycling population of AMPARs. This pathway can be monitored by expressing GluR2-GFP, which has been shown to constitutively reach spine and synaptic compartments (Shi et al., 2001). Therefore, we expressed GluR2-GFP in CA1 hippocampal neurons with or without Exo70-N-RFP, Sec8-Ct-RFP or NR2B-Ct-RFP, as control. Total receptor (GFP channel) and surface (Cy5 channel) distribution of GluR2-GFP was evaluated as described above (see Fig. 5A). As shown in Fig. 6A-C (first and second panels), and similarly to the results obtained with GluR1-GFP, interference with Exo70 function drastically impaired the surface delivery of GluR2 at the spine, and led to a concomitant enrichment of the receptor in the intracellular space of the spine. Interestingly, Sec8-Ct also strongly impaired surface receptor delivery (Fig. 6A, third panel), but this was not accompanied by receptor accumulation within the spine. In fact, Sec8-Ct produced a significant decrease in the fraction of receptors present at spines (Fig. 6B, third panel). As control, NR2B-Ct did not affect receptor presence at spines, and only modestly decreased surface delivery at spines (Fig. 6, forth panels; see also Supplementary Fig. 5 for a comparative analysis of the effects of Sec8-Ct and NR2B-Ct at spine-dendrite pairs).

Taken together, these results indicate that the exocyst plays specialized roles in AMPAR synaptic trafficking, with Sec8 assisting both receptor translocation into the spine and delivery

into the spine surface, while Exo70 mediates exclusively a final membrane fusion step within the spine.

In addition, these results strongly suggest that the exocyst mediates both constitutive and regulated delivery of AMPARs at synapses. As a functional test for the role of the exocyst in these two pathways, we carried out electrophysiological experiments in which the presence of recombinant receptors at synapses is detected from their inward rectification properties (Hayashi et al., 2000; Shi et al., 2001). These electrophysiological experiments reinforced our fluorescence imaging data, and confirmed that the exocyst is required for the functional insertion of all AMPAR populations at synapses (see Supplementary Information).

Distinct roles of Sec8 and Exo70 in targeting and insertion of AMPA receptors at the postsynaptic membrane

In yeast, different subsets of exocyst subunits have been proposed to associate with exocytic vesicles *versus* the target plasma membrane (Boyd et al., 2004). However, it is unknown what exocyst subassemblies reside in each compartment in the case of synaptic trafficking. Furthermore, it is still uncertain whether the target membrane for AMPAR exocytic delivery is directly at the synaptic membrane contained within the postsynaptic density (PSD), or whether AMPARs are inserted in extrasynaptic membranes and then reach their synaptic targets by lateral diffusion (Adesnik et al., 2005; Passafaro et al., 2001; Tardin et al., 2003; Triller and Choquet, 2005). Since Exo70 is required for local surface delivery of AMPARs (Fig. 5 and 6), we then tested whether interference with this exocyst subunit would alter the association of AMPARs with the PSD. To this end, we isolated PSD fractions (protocol based on (Peng et al., 2004); see Supplementary Information) from hippocampal extracts of control slices or slices

overexpressing Exo70-N. To our surprise, and despite the fact that Exo70-N impairs receptor delivery into synapses (Fig. 1D) and spine plasma membrane (Fig. 5 and 6), Exo70-N overexpression led to a marked accumulation of Sec8, Rab8 and AMPARs at the PSD fraction (Fig. 7A and B; to note, none of these proteins is particularly enriched at the PSD fraction under basal conditions). Importantly, endogenous Exo70 and stable components of the PSD, such as PSD95 and αCaMKII, were not affected by expression of Exo70-N (Fig. 7A and B). Another exocytic Rab protein, Rab11, and the small GTPase Rho were undetectable at the PSD fraction under either condition. Therefore, these results together with those monitoring receptor delivery at the spine surface (Fig. 5 and 6), strongly suggest that AMPARs are directly inserted at the postsynaptic membrane (or at membranes biochemically associated to the PSD) in an Exo70-depending manner. Truncation of the Exo70 C-terminus would lead to formation of an abortive complex at the PSD, in which incoming vesicles containing AMPARs, Sec8 and Rab8 remained associated but not yet fused with the postsynaptic membrane.

Importantly, this interpretation also implies that AMPAR targeting towards the postsynaptic membrane does not require a fully functional Exo70. Since Sec8 is the exocyst subunit that interacts with synaptic scaffolding molecules (Riefler et al., 2003; Sans et al., 2003) and it contributes to the transport of AMPARs into spines (Fig. 5), we then tested whether Sec8 may be involved in the targeting aspects of AMPAR delivery into the postsynaptic membrane. To this end, we carried out similar PSD fractionation experiments with hippocampal extracts from uninfected slices, and from slices overexpressing Sec8-Ct. As shown in Fig. 7C and D, Sec8-Ct led to a drastic reduction in the amount of AMPARs and Sec8 at the PSD fraction. Interestingly, the association of NMDARs and PSD95 with the PSD was also decreased, in agreement with the depression of NMDA responses produced by Sec8-Ct (Fig. 1A). The same

result was obtained for the actin-dependent motor protein myosin Va, which is enriched in dendritic spines (Naisbitt et al., 2000; Walikonis et al., 2000). However, Sec8-Ct did not produce a generalized disassembly of the postsynaptic complex since Exo70 and αCaMKII were not affected by Sec8-Ct overexpression. This result with Sec8-Ct is virtually opposite to the one observed with Exo70-N (compare quantifications in Fig. 7B and D), and reinforces the interpretation that Sec8 mediates the targeting of AMPAR-containing vesicles towards the synapse, whereas Exo70 is required for the fusion of these vesicles with the postsynaptic membrane.

Ultrastructural analysis of the role of the exocyst in AMPA receptor insertion at the postsynaptic membrane

The results presented above strongly suggest that AMPARs are able to reach the PSD and accumulate within it when Exo70 function is blocked. In order to test anatomically this interpretation and map with high-spatial resolution the role of Sec8 and Exo70 in AMPAR synaptic insertion, we have carried out immunogold electron microscopy. Organotypic hippocampal slices overexpressing Exo70-N or Sec8-Ct, or control (uninfected) slices were processed for postembedding immunogold staining with anti-GluR2/3 antibodies (see Supplementary Information). Electron micrographs were taken randomly from excitatory (asymmetric) synapses in the stratum radiatum (CA1) of these slices (see representative examples in Fig. 8A). As shown in Fig. 8A, B, AMPAR immunogold particles were significantly enriched (2.6-fold) within the PSD in Exo70-N-expressing slices. In contrast, Sec8-Ct produced a reduction in the fraction of AMPAR labeling at the PSD, although the difference was not significant with respect to uninfected slices.

This result confirms our biochemical observations and strengthens the interpretation that AMPARs approach the postsynaptic membrane but fail to fuse with it in the absence of a functional Exo70. In order to precisely map the trafficking step mediated by Exo70, we measured the distance between each gold particle and the synaptic cleft from slices expressing Exo70-N, Sec8-Ct or uninfected slices. The results are presented as cumulative distributions in Fig. 8C (only gold particles within 60 nm of the synaptic cleft –approximately 3 times the average PSD thickness– were considered for this quantification). As shown in Fig. 8C, AMPARs were found to accumulate in close proximity to the synaptic cleft in slices expressing Exo70-N (red line; leftward shift of the cumulative distribution), even from the shortest measurable distances within the PSD. Sec8-Ct produced the opposite effect, that is, AMPARs were less abundant in the vicinity of the PSD (blue line; rightward sift in the cumulative distribution). These results indicate that, in the absence of functional Exo70, AMPARs approach the postsynaptic membrane as much as physically possible, within the resolution of the immunogold labeling technique.

Since Exo70-N seems to trap AMPARs at their final fusion step with the postsynaptic membrane, we then decided to map where this insertion takes place laterally with respect to the postsynaptic density. To this end we measured the lateral distance to the edge of the PSD for all immungold particles present within the PSD or on the lateral extrasynaptic membrane. As shown in Fig. 8D, in the presence of Exo70-N, AMPARs predominantly accumulate within the PSD, but in close proximity to its edge (almost 40% of the labeling is found within the distal 10% of the PSD) (Sec8-Ct was not included in this analysis due to the low number of gold particles present at the PSD under those conditions). Once again, this analysis supports the interpretation

that AMPARs are inserted into the synaptic membrane directly from the PSD or close to its edge, in a process mediated by the Exo70 subunit of the exocyst.

DISCUSSION

Delivery of AMPARs into synapses requires a precise and continuous coordination between sorting of AMPAR-containing vesicles towards the synapse, and fusion of these incoming vesicles with the postsynaptic membrane. Here we show that the exocyst complex links these two distinct functions through the concerted actions of Sec8 and Exo70. This conclusion is based on four main experimental observations. First, both Sec8 and Exo70 are required for AMPAR function at synapses, as assayed electrophysiologically. Second, both Sec8 and Exo70 dominant negative mutants prevent receptor delivery to the spine surface, but in addition, only blockade of Exo70 function leads to accumulation of AMPARs at intracellular compartments within the spine. Third, exocytic vesicle proteins and AMPARs remain associated with the PSD upon interference with Exo70 function, whereas a Sec8 dominant negative produces the opposite effect. And forth, AMPARs accumulate within the distal part of the PSD in very close proximity to the synaptic cleft when Exo70 function is blocked. These observations lead us to propose a model for the anatomical and molecular events that lead to the delivery of AMPARs into synapses (Fig. 9). First, AMPARs are transported through intracellular membranes, probably belonging to the trans-Golgi network and recycling endosomes (Gerges et al., 2004a; Horton and Ehlers, 2003; Horton and Ehlers, 2004; Park et al., 2004), to reach the spine compartment. This process is constitutive for GluR2/GluR3 receptors, but requires CaMKII activation for GluR1/GluR2 receptors (Piccini and Malinow, 2002). The translocation of AMPARs into the spine is assisted by PDZ-dependent interactions of Sec8, but is independent from the Exo70 subunit of the exocyst. Exocytic vesicles containing AMPARs bud from intra-spine compartments and are targeted towards the postsynaptic density, in a process probably

directed by interactions between the Sec8 subunit of the exocyst and synaptic scaffolding molecules (Fig. 9, left panel). These vesicles dock with the postsynaptic membrane within the PSD, leading to a transient association between AMPARs, vesicular proteins, such as Sec8 and Rab8, and the postsynaptic density (Fig. 9, upper right panel). This step is blocked by Sec8-Ct, presumably by competing with the Sec8-PDZ-dependent interactions that direct the vesicles towards the PSD. Finally, this complex is resolved by exocytic membrane fusion mediated by the Exo70 subunit of the exocyst (Fig 9, lower right panel). The C-terminus of Exo70 is required for this step, since Exo70-N prevents AMPAR delivery into the synaptic surface.

Our results reinforce the current view that different exocyst subunits perform individual functions during the exocytic process (Boyd et al., 2004), with Sec8 being specialized in vesicle transport and targeting, and Exo70 in membrane fusion. More importantly, this model provides new information about the distinct organization of this exocytic machinery in neurons for the delivery of AMPARs at synapses. The exocyst was originally proposed to act as a spatial landmark for polarized exocytosis in yeast (Finger et al., 1998). We now know that the exocyst mediates surface delivery of a variety of membrane proteins in different cell types. Therefore, it is expected that cell- and structure-specific proteins will recruit the exocyst to localize delivery of different cargo to their specific targets. In the case of the synaptic delivery of AMPA receptors, the PDZ-dependent interaction between Sec8 and synaptic scaffolding molecules, such as PSD95, seems to be the determining factor for membrane targeting. This interpretation is consistent with the observation that up- or down-regulation of PSD95 synaptic levels bidirectionally controls AMPAR delivery at synapses in hippocampus (Colledge et al., 2003; Ehrlich and Malinow, 2004; El-Husseini et al., 2000; El-Husseini Ael et al., 2002) and cerebral cortex (Beique and Andrade, 2003)..

Finally, these results have offered unexpected anatomical information about the subcellular pathways followed by AMPARs to reach their synaptic targets. It has been previously proposed that the constitutive delivery of GluR2 receptors occurs by direct insertion at the postsynaptic membrane, whereas GluR1-containg receptors would reach the synaptic membrane by lateral translocation, after being inserted at extrasynaptic membranes (Passafaro et al., 2001). This model is compatible with the reported lateral diffusion of AMPARs on the dendritic plasma membrane (Groc et al., 2004; Tardin et al., 2003). However, our results do not support this model for synaptic delivery. We have found that impairment of AMPAR surface delivery with the Exo70 dominant negative leads to the accumulation of both recombinant GluR1 and GluR2 receptors within the spine, and not in the surrounding dendritic space. Using immunogold electron microscopy, we have shown that endogenous AMPARs accumulate within the PSD, in very close proximity to the synaptic membrane, when Exo70 function is blocked. And finally, AMPARs biochemically associate with PSD fractions when surface delivery is impaired. Taken together, these results strongly suggest that AMPARs are targeted directly into the PSD, but become locked in an abortive complex at its intracellular side when membrane fusion is prevented. We do not know the reason for this discrepancy in the spatial pattern of AMPAR delivery, although a potentially important experimental difference may be the use of organotypic slice cultures in our experiments *versus* dissociated neuronal cultures for the reports on the lateral translocation of AMPARs (see also two recent reports supporting intra-spine delivery in slices (Kopec et al., 2006) and lateral diffusion in dissociated neurons (Adesnik et al., 2005)). Future experiments will be needed to resolve the physiological role of these different delivery pathways.

In conclusion, our results shed light into the complex array of events that coordinate the transport, targeting and insertion of AMPARs at the postsynaptic membrane, and provide a molecular and anatomical map of the intracellular machinery that catalyzes this process along dendrites and within the dendritic spine.

MATERIALS AND METHODS

Electrophysiology

Simultaneous whole-cell recordings were carried out from nearby pairs of infected/transfected and uninfected/untransfected CA1 pyramidal neurons using fluorescence and transmitted light illumination. Synaptic responses were evoked with two bipolar electrodes (stimulation pulses of 200 μs, up to 20 V) placed on the Schaffer collateral fibers between 300 μm and 500 μm of the recorded cell. The responses obtained from the two stimulating electrodes were averaged for each cell and counted as an "n" of 1. This experimental configuration ensures that the potential effects of the expressed recombinant proteins are postsynaptic, since expression is always in CA1 neurons and stimulation is applied on Schaffer collateral fibers from CA3 neurons. Synaptic responses mediated by AMPA or NMDA were acquired at -60 mV or +40 mV, respectively, in the presence of 100 μM picrotoxin to block $GABA_A$ receptors. $GABA_A$ responses were acquired at 0 mV in the absence of receptor antagonists; therefore, they should be considered as a combination of mono- and disynaptic IPSCs. All synaptic responses were averaged over 50-100 trials. Voltage-clamp whole-cell recordings were acquired with a Multiclamp 700A amplifier (Axon Instruments). Composition of perfusion and internal solutions are described in the Supplementary Information.

Imaging

Confocal and electron microscopy experiments are described in the Supplementary Information.

Biochemistry

Biochemical techniques for membrane fractionation and immunoprecipitations from synaptosomal preparations are described in the Supplementary Information.

ACKNOWLEDGMENTS

We thank Alan Saltiel for the plasmids containing the Exo70 and Sec8 coding sequences, Shu-Chan Hsu for the monoclonal antibody against Exo70, Roger Tsien for the red fluorescence protein variant tdimer2(12), Dorothy Sorenson and Chris Edwards for their assistance with the immunogold electron microscopy, members of the Esteban lab and María Soengas for critical reading of the manuscript. This work was supported by grants from the National Institute of Mental Health (grant MH070417) and the National Alliance for Research on Schizophrenia and Depression (NARSAD) to J.A.E, and grant GM63032 from the National Institute of General Medical Sciences to M.R.S. We also thank Dr. Thomas Coles for sponsoring J.A.E. as an Investigator of the National Alliance for the Mentally Ill (NAMI).

REFERENCES

Adesnik, H., Nicoll, R.A. and England, P.M. (2005) Photoinactivation of native AMPA receptors reveals their real-time trafficking. *Neuron*, **48**, 977-985.

Barry, M.F. and Ziff, E.B. (2002) Receptor trafficking and the plasticity of excitatory synapses. *Curr Opin Neurobiol*, **12**, 279-286.

Beique, J.C. and Andrade, R. (2003) PSD-95 regulates synaptic transmission and plasticity in rat cerebral cortex. *J Physiol*, **546**, 859-867.

Boyd, C., Hughes, T., Pypaert, M. and Novick, P. (2004) Vesicles carry most exocyst subunits to exocytic sites marked by the remaining two subunits, Sec3p and Exo70p. *J Cell Biol*, **167**, 889-901.

Bredt, D.S. and Nicoll, R.A. (2003) AMPA receptor trafficking at excitatory synapses. *Neuron*, **40**, 361-379.

Brown, T.C., Tran, I.C., Backos, D.S. and Esteban, J.A. (2005) NMDA receptor-dependent activation of the small GTPase Rab5 drives the removal of synaptic AMPA receptors during hippocampal LTD. *Neuron*, **45**, 81-94.

Colledge, M., Snyder, E.M., Crozier, R.A., Soderling, J.A., Jin, Y., Langeberg, L.K., Lu, H., Bear, M.F. and Scott, J.D. (2003) Ubiquitination regulates PSD-95 degradation and AMPA receptor surface expression. *Neuron*, **40**, 595-607.

Ehrlich, I. and Malinow, R. (2004) Postsynaptic density 95 controls AMPA receptor incorporation during long-term potentiation and experience-driven synaptic plasticity. *J Neurosci*, **24**, 916-927.

El-Husseini, A.E., Schnell, E., Chetkovich, D.M., Nicoll, R.A. and Bredt, D.S. (2000) PSD-95 involvement in maturation of excitatory synapses. *Science*, **290**, 1364-1368.

El-Husseini Ael, D., Schnell, E., Dakoji, S., Sweeney, N., Zhou, Q., Prange, O., Gauthier-Campbell, C., Aguilera-Moreno, A., Nicoll, R.A. and Bredt, D.S. (2002) Synaptic strength regulated by palmitate cycling on PSD-95. *Cell*, **108**, 849-863.

Esteban, J.A. (2003) AMPA receptor trafficking: a road map for synaptic plasticity. *Mol Interv*, **3**, 375-385.

Finger, F.P., Hughes, T.E. and Novick, P. (1998) Sec3p is a spatial landmark for polarized secretion in budding yeast. *Cell*, **92**, 559-571.

Garner, C.C., Nash, J. and Huganir, R.L. (2000) PDZ domains in synapse assembly and signalling. *Trends Cell Biol*, **10**, 274-280.

Gerges, N.Z., Backos, D.S. and Esteban, J.A. (2004a) Local control of AMPA receptor trafficking at the postsynaptic terminal by a small GTPase of the Rab family. *J Biol Chem*, **279**, 43870-43878.

Gerges, N.Z., Tran, I.C., Backos, D.S., Harrell, J.M., Chinkers, M., Pratt, W.B. and Esteban, J.A. (2004b) Independent functions of hsp90 in neurotransmitter release and in the continuous synaptic cycling of AMPA receptors. *J Neurosci*, **24**, 4758-4766.

Groc, L., Heine, M., Cognet, L., Brickley, K., Stephenson, F.A., Lounis, B. and Choquet, D. (2004) Differential activity-dependent regulation of the lateral mobilities of AMPA and NMDA receptors. *Nat Neurosci*, **7**, 695-696.

Hayashi, Y., Shi, S.H., Esteban, J.A., Piccini, A., Poncer, J.C. and Malinow, R. (2000) Driving AMPA receptors into synapses by LTP and CaMKII: requirement for GluR1 and PDZ domain interaction. *Science*, **287**, 2262-2267.

Hazuka, C.D., Foletti, D.L., Hsu, S.C., Kee, Y., Hopf, F.W. and Scheller, R.H. (1999) The sec6/8 complex is located at neurite outgrowth and axonal synapse-assembly domains. *J Neurosci*, **19**, 1324-1334.

Henley, J.M. (2003) Proteins interactions implicated in AMPA receptor trafficking: a clear destination and an improving route map. *Neurosci Res*, **45**, 243-254.

Horton, A.C. and Ehlers, M.D. (2003) Dual modes of endoplasmic reticulum-to-Golgi transport in dendrites revealed by live-cell imaging. *J Neurosci*, **23**, 6188-6199.

Horton, A.C. and Ehlers, M.D. (2004) Secretory trafficking in neuronal dendrites. *Nat Cell Biol*, **6**, 585-591.

Hsu, S.C., Hazuka, C.D., Roth, R., Foletti, D.L., Heuser, J. and Scheller, R.H. (1998) Subunit composition, protein interactions, and structures of the mammalian brain sec6/8 complex and septin filaments. *Neuron*, **20**, 1111-1122.

Hsu, S.C., Ting, A.E., Hazuka, C.D., Davanger, S., Kenny, J.W., Kee, Y. and Scheller, R.H. (1996) The mammalian brain rsec6/8 complex. *Neuron*, **17**, 1209-1219.

Inoue, M., Chang, L., Hwang, J., Chiang, S.H. and Saltiel, A.R. (2003) The exocyst complex is required for targeting of Glut4 to the plasma membrane by insulin. *Nature*, **422**, 629-633.

Kee, Y., Yoo, J.S., Hazuka, C.D., Peterson, K.E., Hsu, S.C. and Scheller, R.H. (1997) Subunit structure of the mammalian exocyst complex. *Proc Natl Acad Sci U S A*, **94**, 14438-14443.

Kim, E. and Sheng, M. (2004) PDZ domain proteins of synapses. *Nat Rev Neurosci*, **5**, 771-781.

Kopec, C.D., Li, B., Wei, W., Boehm, J. and Malinow, R. (2006) Glutamate receptor exocytosis and spine enlargement during chemically induced long-term potentiation. *J Neurosci*, **26**, 2000-2009.

Kornau, H.C., Schenker, L.T., Kennedy, M.B. and Seeburg, P.H. (1995) Domain interaction between NMDA receptor subunits and the postsynaptic density protein PSD-95. *Science*, **269**, 1737-1740.

Luscher, C., Xia, H., Beattie, E.C., Carroll, R.C., von Zastrow, M., Malenka, R.C. and Nicoll, R.A. (1999) Role of AMPA receptor cycling in synaptic transmission and plasticity. *Neuron*, **24**, 649-658.

Malinow, R. and Malenka, R.C. (2002) AMPA receptor trafficking and synaptic plasticity. *Annu Rev Neurosci*, **25**, 103-126.

McGee, A.W. and Bredt, D.S. (2003) Assembly and plasticity of the glutamatergic postsynaptic specialization. *Curr Opin Neurobiol*, **13**, 111-118.

Naisbitt, S., Valtschanoff, J., Allison, D.W., Sala, C., Kim, E., Craig, A.M., Weinberg, R.J. and Sheng, M. (2000) Interaction of the postsynaptic density-95/guanylate kinase domain-associated protein complex with a light chain of myosin-V and dynein. *J Neurosci*, **20**, 4524-4534.

Niethammer, M., Kim, E. and Sheng, M. (1996) Interaction between the C terminus of NMDA receptor subunits and multiple members of the PSD-95 family of membrane-associated guanylate kinases. *J Neurosci*, **16**, 2157-2163.

Nishimune, A., Isaac, J.T., Molnar, E., Noel, J., Nash, S.R., Tagaya, M., Collingridge, G.L., Nakanishi, S. and Henley, J.M. (1998) NSF binding to GluR2 regulates synaptic transmission. *Neuron*, **21**, 87-97.

Nong, Y., Huang, Y.Q. and Salter, M.W. (2004) NMDA receptors are movin' in. *Curr Opin Neurobiol*, **14**, 353-361.

Park, M., Penick, E.C., Edwards, J.G., Kauer, J.A. and Ehlers, M.D. (2004) Recycling endosomes supply AMPA receptors for LTP. *Science*, **305**, 1972-1975.

Passafaro, M., Piech, V. and Sheng, M. (2001) Subunit-specific temporal and spatial patterns of AMPA receptor exocytosis in hippocampal neurons. *Nat Neurosci*, **4**, 917-926.

Peng, J., Kim, M.J., Cheng, D., Duong, D.M., Gygi, S.P. and Sheng, M. (2004) Semi-quantitative proteomic analysis of rat forebrain postsynaptic density fractions by mass spectrometry. *J Biol Chem*.

Perez-Otano, I. and Ehlers, M.D. (2005) Homeostatic plasticity and NMDA receptor trafficking. *Trends Neurosci*, **28**, 229-238.

Piccini, A. and Malinow, R. (2002) Critical postsynaptic density 95/disc large/zonula occludens-1 interactions by glutamate receptor 1 (GluR1) and GluR2 required at different subcellular sites. *J Neurosci*, **22**, 5387-5392.

Prybylowski, K., Chang, K., Sans, N., Kan, L., Vicini, S. and Wenthold, R.J. (2005) The Synaptic Localization of NR2B-Containing NMDA Receptors Is Controlled by Interactions with PDZ Proteins and AP-2. *Neuron*, **47**, 845-857.

Riefler, G.M., Balasingam, G., Lucas, K.G., Wang, S., Hsu, S.C. and Firestein, B.L. (2003) Exocyst complex subunit sec8 binds to postsynaptic density protein-95 (PSD-95): a novel interaction regulated by cypin (cytosolic PSD-95 interactor). *Biochem J*, **373**, 49-55.

Sans, N., Petralia, R.S., Wang, Y.X., Blahos, J., 2nd, Hell, J.W. and Wenthold, R.J. (2000) A developmental change in NMDA receptor-associated proteins at hippocampal synapses. *J Neurosci*, **20**, 1260-1271.

Sans, N., Prybylowski, K., Petralia, R.S., Chang, K., Wang, Y.X., Racca, C., Vicini, S. and Wenthold, R.J. (2003) NMDA receptor trafficking through an interaction between PDZ proteins and the exocyst complex. *Nat Cell Biol*, **5**, 520-530.

Scannevin, R.H. and Huganir, R.L. (2000) Postsynaptic organization and regulation of excitatory synapses. *Nat Rev Neurosci*, **1**, 133-141.

Sheng, M. (2001) Molecular organization of the postsynaptic specialization. *Proc Natl Acad Sci U S A*, **98**, 7058-7061.

Sheng, M. and Lee, S.H. (2001) AMPA receptor trafficking and the control of synaptic transmission. *Cell*, **105**, 825-828.

Shi, S., Hayashi, Y., Esteban, J.A. and Malinow, R. (2001) Subunit-specific rules governing AMPA receptor trafficking to synapses in hippocampal pyramidal neurons. *Cell*, **105**, 331-343.

Shin, D.M., Zhao, X.S., Zeng, W., Mozhayeva, M. and Muallem, S. (2000) The mammalian Sec6/8 complex interacts with Ca(2+) signaling complexes and regulates their activity. *J Cell Biol*, **150**, 1101-1112.

Song, I., Kamboj, S., Xia, J., Dong, H., Liao, D. and Huganir, R.L. (1998) Interaction of the N-ethylmaleimide-sensitive factor with AMPA receptors. *Neuron*, **21**, 393-400.

Steiner, P., Alberi, S., Kulangara, K., Yersin, A., Sarria, J.C., Regulier, E., Kasas, S., Dietler, G., Muller, D., Catsicas, S. and Hirling, H. (2005) Interactions between NEEP21, GRIP1 and GluR2 regulate sorting and recycling of the glutamate receptor subunit GluR2. *Embo J*, **24**, 2873-2884.

Tardin, C., Cognet, L., Bats, C., Lounis, B. and Choquet, D. (2003) Direct imaging of lateral movements of AMPA receptors inside synapses. *Embo J*, **22**, 4656-4665.

TerBush, D.R., Maurice, T., Roth, D. and Novick, P. (1996) The Exocyst is a multiprotein complex required for exocytosis in Saccharomyces cerevisiae. *Embo J*, **15**, 6483-6494.

Ting, A.E., Hazuka, C.D., Hsu, S.C., Kirk, M.D., Bean, A.J. and Scheller, R.H. (1995) rSec6 and rSec8, mammalian homologs of yeast proteins essential for secretion. *Proc Natl Acad Sci U S A*, **92**, 9613-9617.

Triller, A. and Choquet, D. (2005) Surface trafficking of receptors between synaptic and extrasynaptic membranes: and yet they do move! *Trends Neurosci*, **28**, 133-139.

Vega, I.E. and Hsu, S.C. (2001) The exocyst complex associates with microtubules to mediate vesicle targeting and neurite outgrowth. *J Neurosci*, **21**, 3839-3848.

Vik-Mo, E.O., Oltedal, L., Hoivik, E.A., Kleivdal, H., Eidet, J. and Davanger, S. (2003) Sec6 is localized to the plasma membrane of mature synaptic terminals and is transported with secretogranin II-containing vesicles. *Neuroscience*, **119**, 73-85.

Walikonis, R.S., Jensen, O.N., Mann, M., Provance, D.W., Jr., Mercer, J.A. and Kennedy, M.B. (2000) Identification of proteins in the postsynaptic density fraction by mass spectrometry. *J Neurosci*, **20**, 4069-4080.

Wang, S., Liu, Y., Adamson, C.L., Valdez, G., Guo, W. and Hsu, S.C. (2004) The mammalian exocyst, a complex required for exocytosis, inhibits tubulin polymerization. *J Biol Chem*, **279**, 35958-35966.

Wyszynski, M., Valtschanoff, J.G., Naisbitt, S., Dunah, A.W., Kim, E., Standaert, D.G., Weinberg, R. and Sheng, M. (1999) Association of AMPA receptors with a subset of glutamate receptor-interacting protein in vivo. *J Neurosci*, **19**, 6528-6537.

Yamagata, M., Sanes, J.R. and Weiner, J.A. (2003) Synaptic adhesion molecules. *Curr Opin Cell Biol*, **15**, 621-632.

Yeaman, C., Grindstaff, K.K., Wright, J.R. and Nelson, W.J. (2001) Sec6/8 complexes on trans-Golgi network and plasma membrane regulate late stages of exocytosis in mammalian cells. *J Cell Biol*, **155**, 593-604.

FIGURE LEGENDS

Figure 1. Effect of different exocyst subunits on synaptic transmission. (**A-E**) Insets, sample trace of evoked AMPA-receptor mediated synaptic responses recorded at –60 mV, from uninfected and infected cells. Scale bars, 20 pA and 40 ms. **Left**: average AMPAR-mediated current amplitude (i.e. the peak of the response recorded at –60 mV) from infected (inf) neurons expressing Sec8-Ct (A), Sec8-wt (B), Sec8-Ct-Δ4 (C), Exo70-N (D) or Exo70-wt (E), and control neighboring cells not expressing the recombinant protein (uninf). n represents the number of cell pairs. **Middle**: average NMDAR-mediated current amplitude (recorded at +40 mV at a latency when AMPA responses are fully decayed, 60 ms) from uninfected and infected cells (n also represents the number of cell pairs). **Right**: average $GABA_A$ receptor-mediated current amplitude measured at 0 mV (A) or average AMPA/NMDA ratios for uninfected and infected cells (B-E).

Figure 2. Interference of the constitutive synaptic cycling of AMPA receptors with a Sec8 C-t peptide. (**A**) Time course of AMPAR-mediated responses recorded from CA1 neurons during whole-cell pipette infusion of Sec8 C-t, NR2B C-t or Sec8-mut C-t peptides, as indicated. Responses are normalized to a 2-minute baseline from the beginning of the recording. The statistical significance of the run-down of AMPA transmission was calculated from the last 5 minutes of the recordings. (**B**) Time course of the pipette access resistance during the recordings shown in A. There was no systematic change in access resistance with any of the peptides.

Figure 3. Co-immunoprecipitation of exocyst subunits and AMPA receptors from hippocampal synaptosomes. Exocyst subunits Exo70 and Sec8 (**A**), AMPA receptor subunits

GluR2/3 (GR2/3) and NMDA receptor subunit NR1 (**B**) were immunoprecipitated from Triton-solubilized synaptosomal preparation of hippocampus. IP indicates antibodies used for immunoprecipitation. Non-immune (N.I.) antibodies were used as control. Total solubilized protein (10% of the input) and the immunoprecipitated fractions were analyzed by immunoblotting using the indicated antibodies.

Figure 4. Exo70 is not involved in the dendritic trafficking of newly synthesized AMPA receptors in hippocampal slices. Hippocampal CA1 neurons were transfected with GluR2-GFP alone or cotransfected with GluR2-GFP plus Exo70-N-RFP, Sec8-Ct-RFP or NR2B-Ct-RFP (these constructs are equivalent to their GFP counterparts, only with RFP in the place of GFP; the NR2B construct includes the last 16 amino acids of the NR2B C-terminus). (**A**) Representative examples of neurons expressing GluR2-GFP alone or co-expressing GluR2-GFP together with Exo70-N-RFP or with Sec8-Ct-RFP, as indicated. Scale bar: 20 μm. The efficiency of GluR2 transport along dendrites was quantified from the intensity of GFP fluorescence at the main apical dendrite 170 to 200 μm away from the cell soma. Fluorescence intensity is normalized to the peak value at the soma after background subtraction (see arrows on left panel and representative scheme in Supplementary Fig. 4A). (**B**) GluR2-GFP presence at distal apical dendrites (170 to 200 μm away from the cell soma) in the presence of Exo70-N, Sec8-Ct or NR2B-Ct, as indicated. Data are presented as mean ± s.e.m. n represents number of cells.

Figure 5. Role of Exo70 in local AMPAR trafficking at spines. (**A**) Representative confocal image of a spine and the adjacent dendritic shaft from a neuron transfected with GluR1-GFP and

tCaMKII (left) or with GluR1-GFP, tCaMKII and Exo70-N-RFP (right), as indicated. GFP fluorescence signal (green) represents total GluR1 receptor distribution. Surface GluR1-GFP receptor (cyan) was assayed by immunostaining with an anti-GFP antibody coupled to Cy5 under non-permeabilized conditions. Scale bar: 2 μm. Lower panels: representative line plot profiles of GFP and Cy5 fluorescence intensities across dendrite-spine pairs. Total (GFP) and surface (Cy5) receptor accumulation are calculated from the corresponding peaks of fluorescence intensity at spines and adjacent dendritic shafts. (**B**) Surface analysis (background-subtracted Cy5 values) from pairs of spines and dendrites in GluR1 plus tCaMKII transfected neurons (first panel; n=59 spine/dendrite pairs from 5 different cells) or in GluR1 plus tCaMKII and Exo70-N cotransfected neurons (second panel; n=40 spine/dendrite pairs from 5 different cells). Surface values are normalized by the mean dendrite value. Cumulative probabilities (third panel) of surface expression at spine over dendrite show significant differences between surface distributions of GluR1 plus tCaMKII *versus* GluR1 plus tCaMKII and Exo70-N transfected neurons. (**C**) Total receptor amount (GFP signal) in spines and dendrites are calculated in GluR1 plus tCaMKII transfected neurons and in neurons co-transfected with GluR1 plus tCaMKII and Exo70-N, as indicated. GFP fluorescence is normalized to the mean dendrite value. The cumulative probability (right) indicates that Exo70-N leads to the accumulation of total receptor in spines as compared to dendrites. (**D**) Surface ratio from the same pairs of spines and dendrites. Surface ratios were calculated by dividing the corresponding background-subtracted Cy5 and GFP values. Surface ratios are normalized by the mean dendrite value. Cumulative probabilities (right) of spine/dendrite ratios show a significant difference between the surface ratio distribution of GluR1 plus tCaMKII *versus* GluR1 plus tCaMKII and Exo70-N transfected neurons.

Figure 6. Role of Exo70 and Sec8 in the constitutive AMPAR trafficking at spines. (**A**) Similar to Fig. 5B, surface analysis from pairs of spines and dendrites in GluR2 (first panel; n=21 spine/dendrite pairs from 4 different cells), GluR2 plus Exo70-N (second panel; n=32 spine/dendrite pairs from 5 different cells), GluR2 plus Sec8-Ct (third panel; n=58 spine/dendrite pairs from 5 different cells) or GluR2 plus NR2B-Ct cotransfected neurons (forth panel; n=62 spine/dendrite pairs from 5 different cells). (**B**) Similar to Fig. 5C, total receptor amount from the same pairs of spines and dendrites in GluR2 or in GluR2 plus Exo70-N, Sec8-Ct or NR2B-Ct cotransfected neurons. (**C**) Similar to Fig. 5D, surface ratio of the same pairs of spines and dendrites in GluR2 or in GluR2 plus Exo70-N, Sec8-Ct or NR2B-Ct cotransfected neurons.

Figure 7. Opposite effects of Exo70 and Sec8 dominant negatives in the association of AMPA receptors with the postsynaptic density. (**A**) Total proteins in synaptosomes (8% of the total fraction) and PSD-associated proteins were analyzed by immunoblotting using the indicated antibodies (AMPARs were detected with a mix of GluR1 and GluR2/3 antibodies). The CA1 area was dissected from 30-45 control (unin.) hippocampal slices or slices infected with Exo70-N (inf.). Therefore, an "n" of 1 in this experiment represents the average of 30-45 slices. Protein extracts were processed to isolate the synaptosomal and PSD fractions (see Supplementary Information). (**B**) Quantification of multiple independent experiments as the one shown in A. Relative PSD enrichment was calculated as the intensity of the PSD band in the infected extracts over that of the uninfected ones, after normalization by their relative band intensities at the homogenates (input). Inset shows that infection did not produce a systematic effect on protein abundance at the inputs. (**C**) Similar to (A), comparing uninfected and infected slices expressing Sec8-Ct (same construct as in Fig. 1). Total proteins in synaptosomes (3% of the total fraction)

and PSD-associated proteins were analyzed by immunoblotting using the indicated antibodies. NMDARs were detected with a combination of NR1 and NR2A/B antibodies). (**D**). Quantification of PSD enrichment for the different proteins in the presence or absence of Sec8-Ct was calculated as described for (B).

Figure 8. Electron microscopic analysis of the role of the exocyst in AMPA receptor synaptic insertion. A. Representative micrographs of AMPA receptor immunogold labeling in control slices (Uninf), slices infected with Exo70 dominant negative (Exo70-N) or with Sec8 dominant negative (Sec8-Ct; same construct as in Fig. 1). Immunogold particles at the postsynaptic density (PSD) are indicated with arrows. Note accumulation of AMPA receptors within the PSD in Exo70-N-expressing neurons. The opposite effect was observed in Sec8-Ct-infected slices. **B.** Quantification of AMPA receptor presence at the PSD from electron micrographs as the ones shown in A. Percentage of PSD labeling was calculated as the number of gold particles at the PSD versus the total number of gold particles in each synaptic terminal (only gold particles within 800 nm of the synaptic cleft were included for quantification). n represents the number of synapses analyzed in each condition. **C.** Quantification of AMPA receptor local distribution with respect to the synaptic cleft. The distance to the synaptic cleft was calculated for each immunogold particle from uninfected slices (black line), slices expressing Exo70-N (red line) or Sec8-Ct (blue line), and plotted as cumulative distributions. In order to assess local synaptic distribution of AMPA receptors, only immunogold particles within 60 nm of the synaptic cleft were included in this quantification (the average thickness of the PSD from our micrographs was 18 nm –thick line on the x-axis). n represents the number of gold particles analyzed in each condition. **D.** Quantification of AMPA receptor lateral distribution

within the PSD and on extrasynaptic membranes from uninfected slices (white columns) and Exo70-N-expressing slices (red columns). The lateral distance to the closest edge of the PSD was calculated for each immunogold particle and divided by the total length of the PSD (the average length of the PSD from our micrographs was 290 nm). Distances within the PSD were computed as negative values (relative lateral distances within the PSD cannot exceed -0.5, since the position of the immunogold particle is always calculated with respect to the closest PSD edge).

Figure 9. Model for the exocyst-mediated targeting and delivery of AMPA receptors at the postsynaptic membrane. Left. Exocytic vesicles containing AMPA receptors reach dendritic spines, bud from intracellular compartments within the spine and are directed towards the PSD by interactions between Sec8 and synaptic scaffolding molecules, such as PSD95. **Upper right.** Incoming vesicles dock at the PSD forming a transient complex with it. **Lower right.** This complex is resolved by membrane fusion with the postsynaptic membrane. This process is mediated by Exo70. See further explanation in the main text. TGN: trans-Golgi network; RE: recycling endosome; EV: exocytic vesicle; DV: docked vesicle.

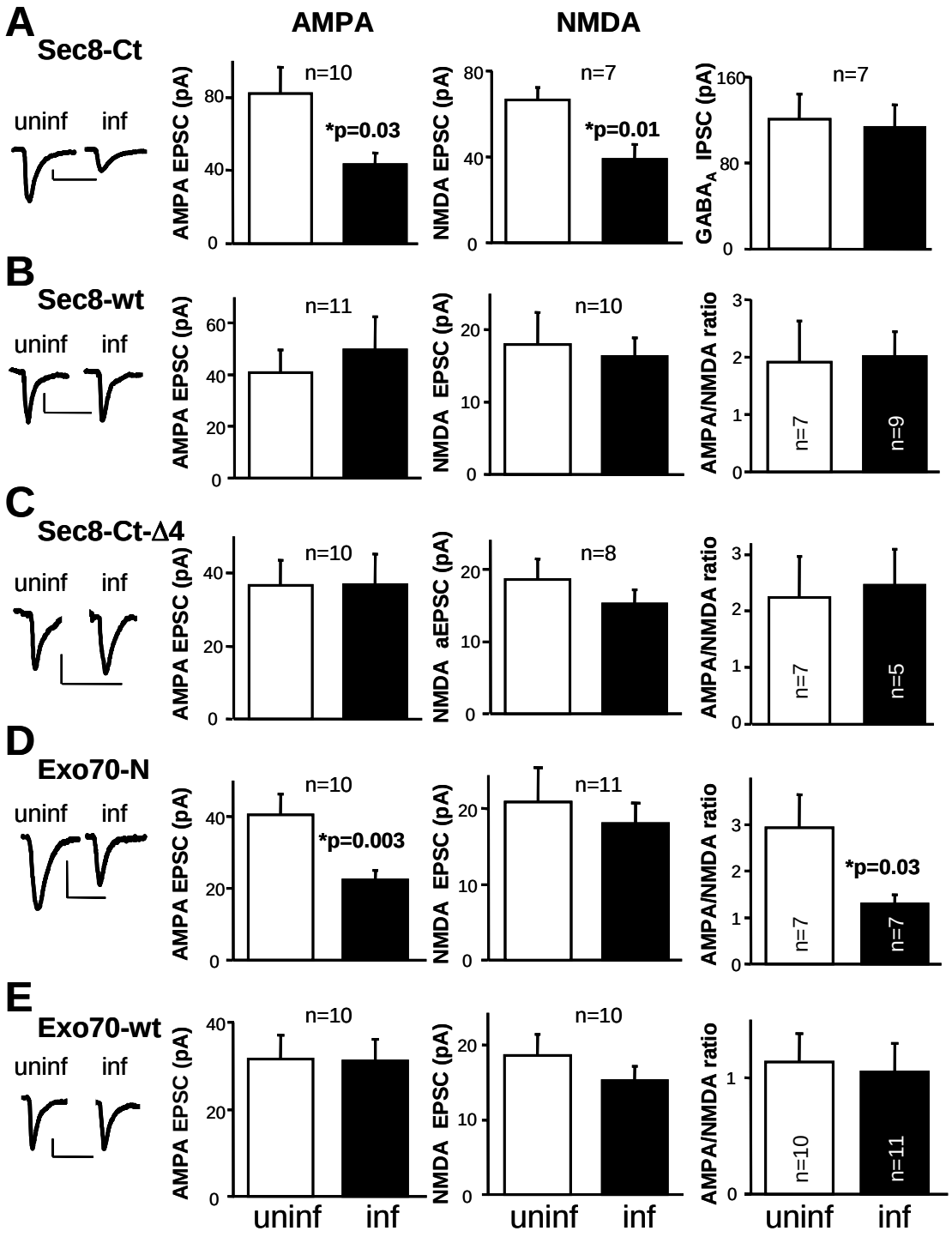

Figure 1 (Esteban)

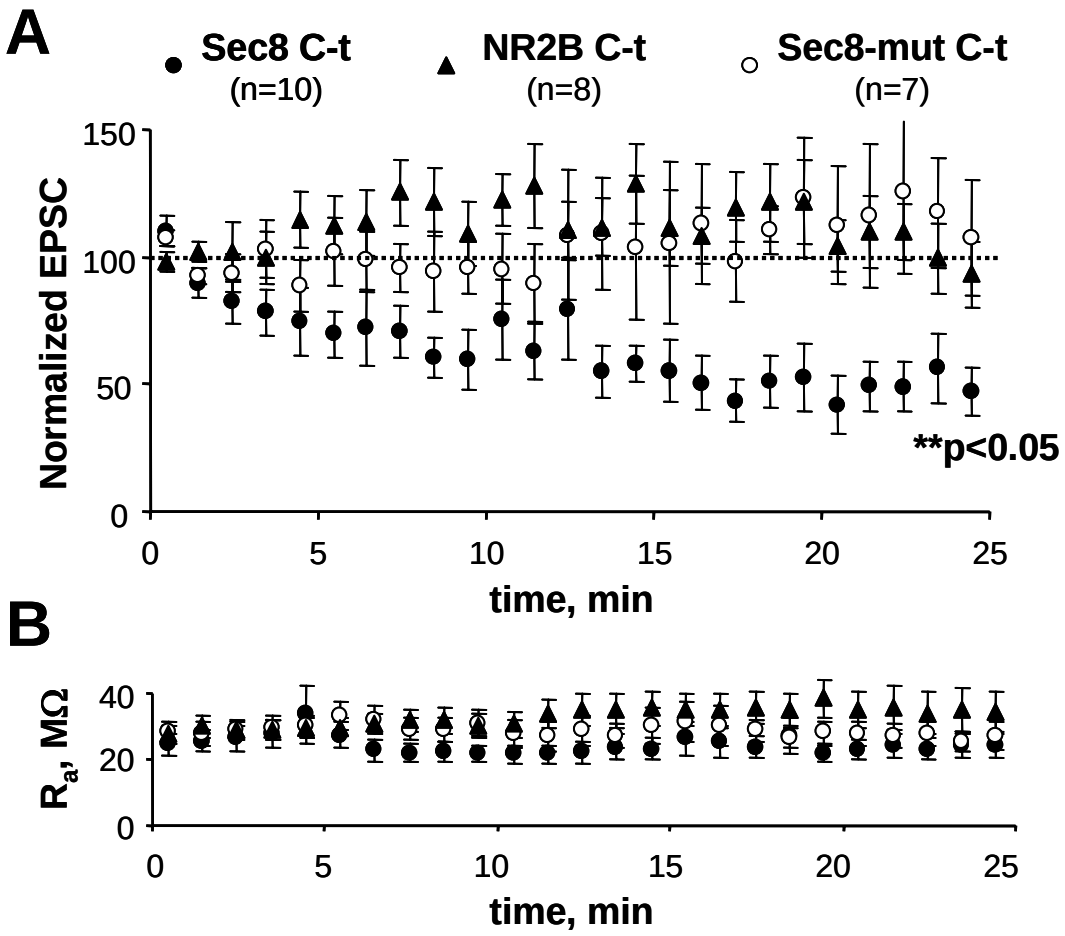

Figure 2 (Esteban)

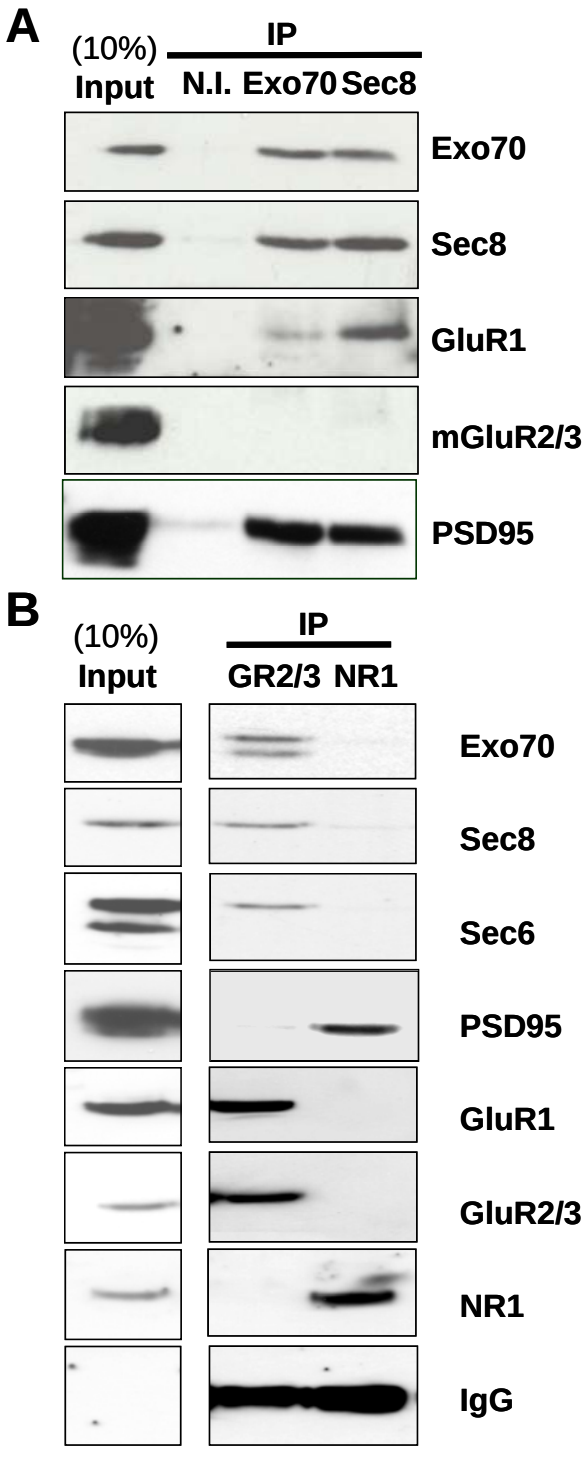

Figure 3 (Esteban)

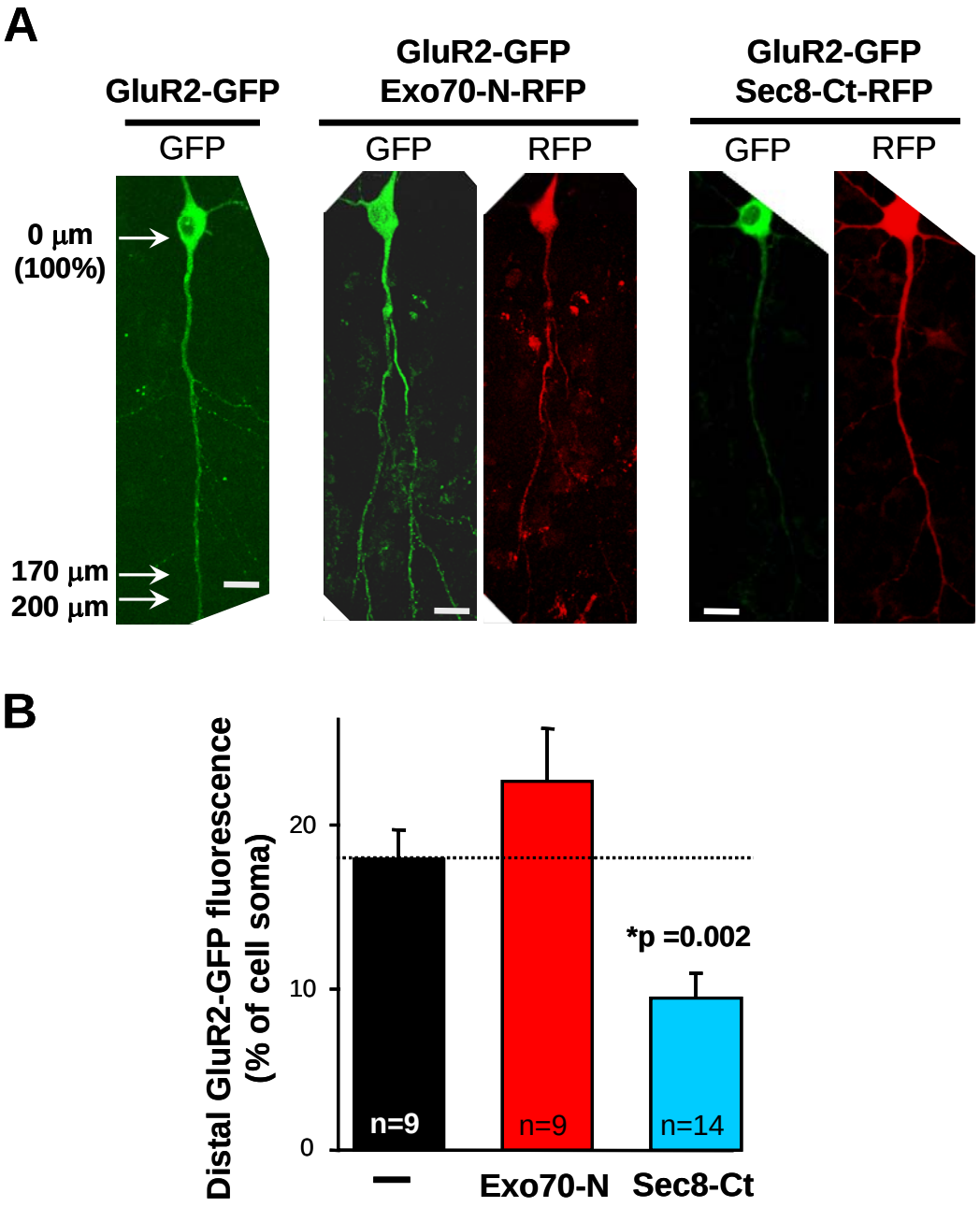

Figure 4 (Esteban)

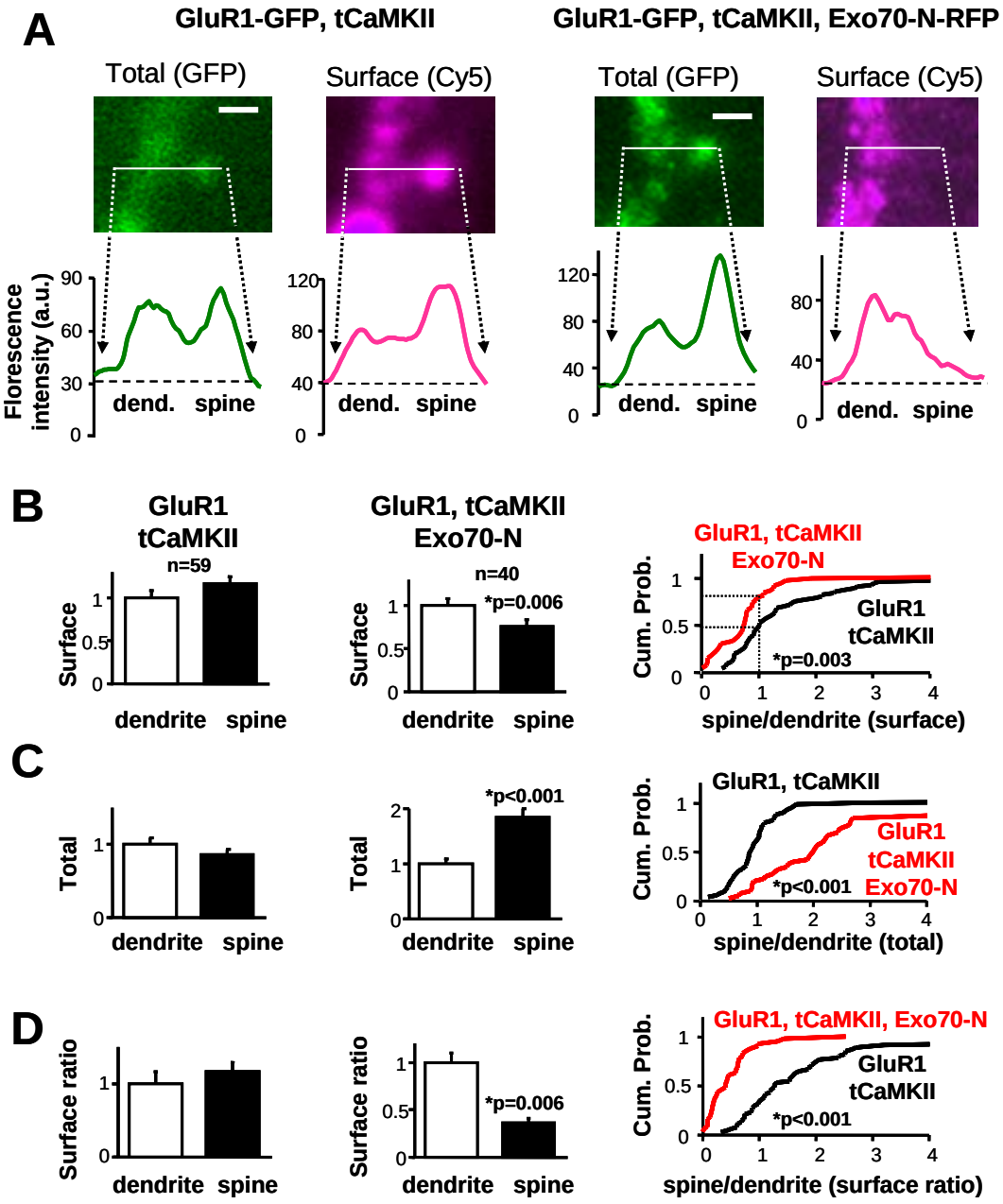

Figure 5 (Esteban)

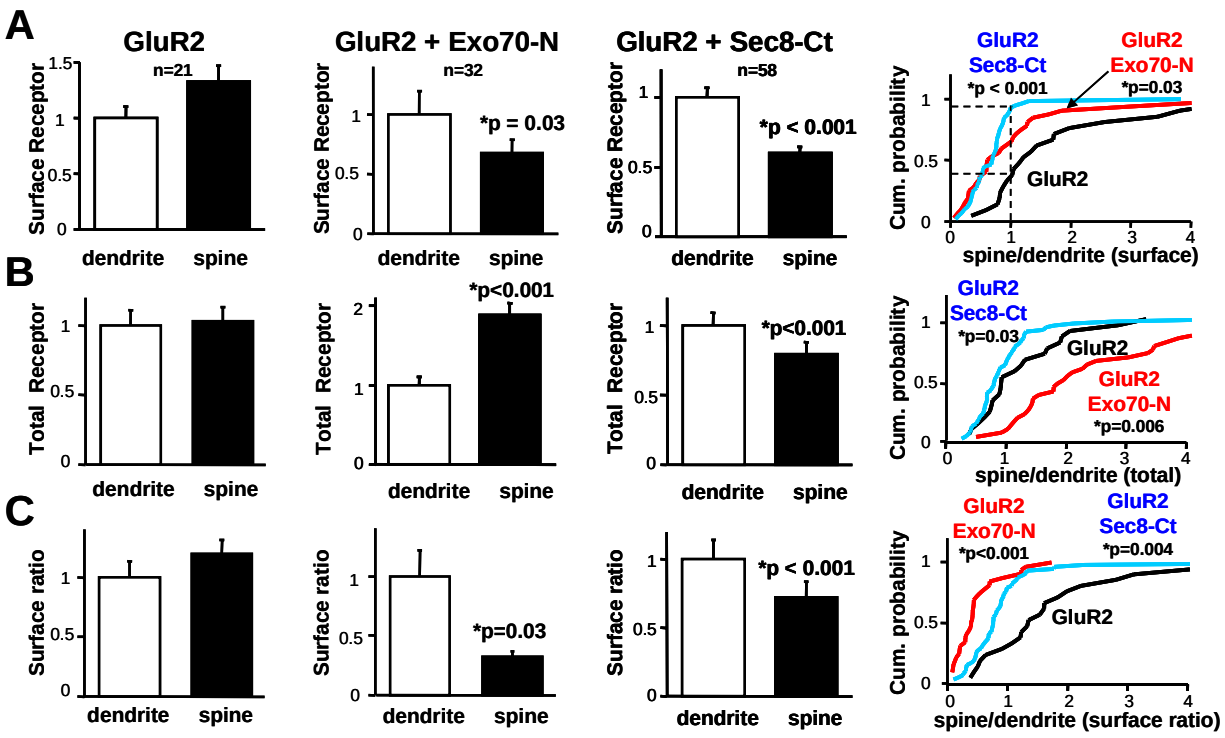

Figure 6 (Esteban)

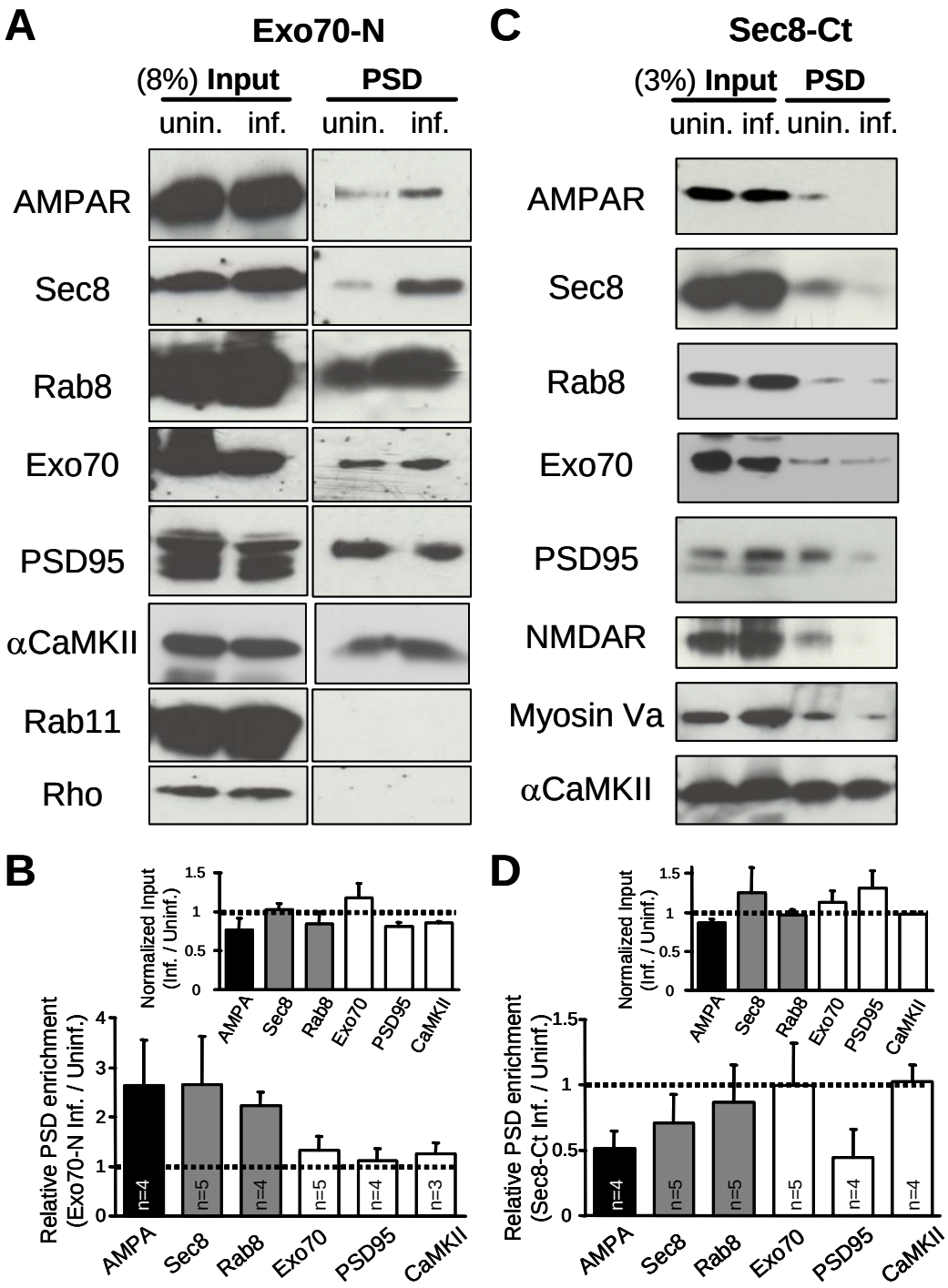

Figure 7 (Esteban)

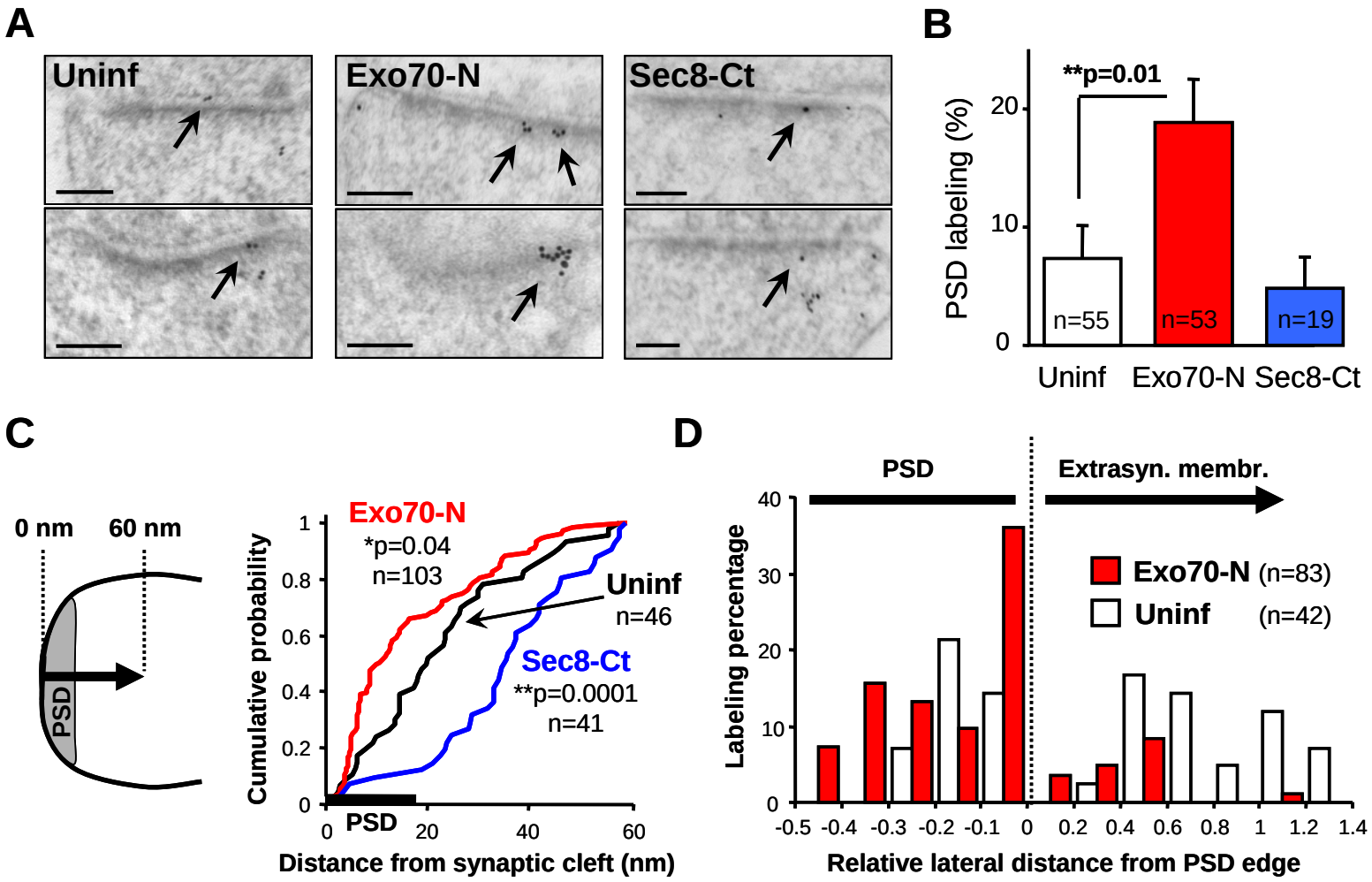

Figure 8 (Esteban)

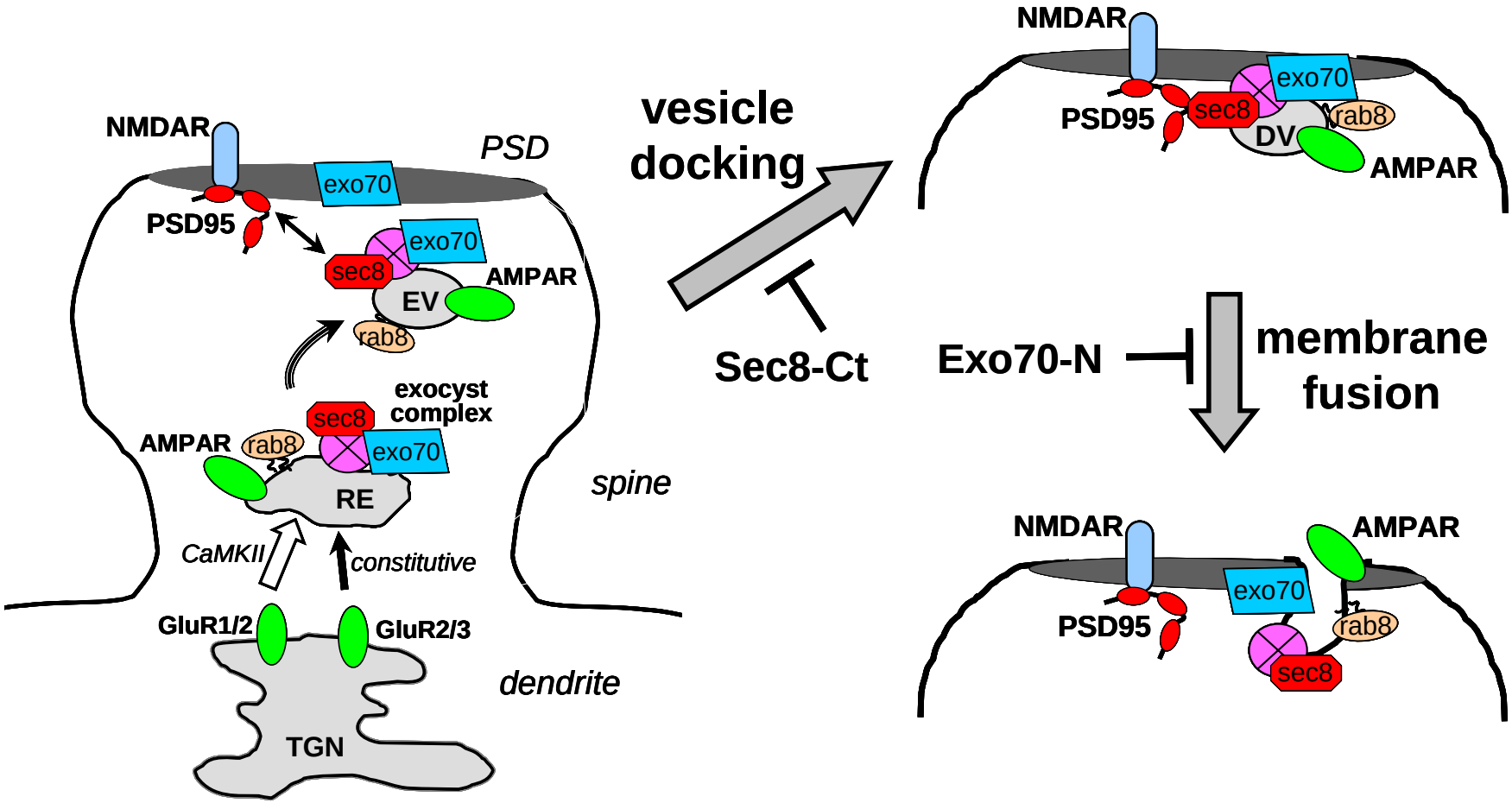

Figure 9 (Esteban)